

# Fraunhofer-type diffraction patterns of matter-wave scattering of projectiles: Electron transfer in energetic ion-atom collisions

Hicham Agueny

*Sorbonne Universités, UPMC Univ Paris 06, UMR 7614,**Laboratoire de Chimie Physique-Matière et Rayonnement, F-75231 Paris Cedex 05, France;**UFR de Physique du Rayonnement et des Interactions Laser-Matière,**Faculté des Sciences, Université Moulay Ismail, B.P. 11201, Zitoune, Meknès, Morocco;**and Department of Physics and Technology, Allegt. 55, University of Bergen, N-5007 Bergen, Norway*

(Received 1 April 2015; published 10 July 2015)

We present results for single and double electron captures in intermediate energies  $H^+$  and  $He^{2+}$  projectiles colliding with a helium target. The processes under investigations are treated using a nonperturbative semiclassical approach in combination with Eikonal approximation to calculate the scattering differential cross sections. The latter reveals pronounced minima and maxima in the scattering angles, in excellent agreement with the recent experimental data. It turns out that the present structure depends strongly on the projectile energy and shows only slight variations with different capture channels. The observed structure demonstrates the analogy of atomic de Broglie's matter-wave scattering with  $\lambda_{dB} = 1.3\text{--}3.2 \times 10^{-3}$  a.u. and Fraunhofer-type diffraction of light waves.

DOI: [10.1103/PhysRevA.92.012702](https://doi.org/10.1103/PhysRevA.92.012702)

PACS number(s): 34.10.+x, 34.50.-s, 34.70.+e

## I. INTRODUCTION

Interference patterns observed during different electronic processes induced in the collisions between ions and diatomic molecules have been extensively investigated as analogous to the seminal Young's double slit experiment (see Refs. [1–3] and references therein). It turns out, however, that a similar pattern can be observed in the scattering from an atom, which behaves like a single slit, instead of a diatomic molecule. This is well known in classical optics by Fraunhofer-type diffraction. The latter is observed when light is diffracted by a circular aperture in an infinite screen and interpreted generally as resulting from the coherent superposition and interference of waves propagating via different paths through the diffracting region.

In atomic collisions, a deeper understanding of the electron transfer collision dynamics requires study of the scattering differential cross sections (SDCSs), which provide, in addition, more detailed information about the dynamical stage between the collision partners. In that context, such an analysis of SDCSs in terms of Fraunhofer diffraction of matter waves from atomic targets has not received much attention except for some experimental works [4–8]. The first experimental observations of such phenomena were made by Van der Poel *et al.* [4,5] for slow  $Li^+$ -Na single electron-capture collisions. Clear oscillation structures were observed in the angular distribution of projectile, and good agreement with predictions of the semiclassical impact-parameter method was found. The phenomenon was attributed to Fraunhofer diffraction of the matter waves. The same phenomenon has been revealed recently in the measured differential cross sections at intermediate [6,8] and higher energies of the projectile [7]. However, to our knowledge no theoretical investigations of such phenomena have been reported in two-electron processes to actively take part in the collision dynamics.

Under the framework of these two-electron processes, previous theoretical calculations of SDCSs mainly focused on small [9,10] or higher [11–15] energies of the projectile. At small energies, electron transfer proceeds via the formation

of the transient molecule formed by the passing projectile and the atomic target, and the SDCSs show oscillation structures depending on scattering angles [16]. Such structures have been interpreted as arising due to different reaction paths associated with the branching pseudocrossing of the potential curves. This is well known as Stueckelberg-type oscillations (see Ref. [17] for an overview of more analysis of these structures). At higher energies, electron transfer is more likely governed by a classical Thomas process [18] characterized by a clear peak in the SDCS near the Thomas angle of 0.47 mrad [7,19–21]. In this picture, an electron is accelerated to the swift projectile ion, and then this electron gets scattered off the target nucleus such that it propagates toward the projectile and gets captured. At intermediate energies, most of the theoretical investigations are limited to the independent electrons model [22] or based on a perturbation approach [23–26] in which a serious disagreement with experiment was found. Such studies in this energy range remain a challenge, since this requires us to take into account different coupling open channels, including electron capture, excitation, ionization, and all multielectronic processes taking into account the electron-electron correlations.

Recently SDCSs for electron transfer at intermediate energies (25–75 keV/u)  $H^+/He^{2+} + He$  collisions have been studied both experimentally and theoretically. The latter exhibits a certain structure at small scattering angles, and its origin has been widely discussed [22–31]. Although many suggestions have been evoked either in terms of quantum-mechanical description of the nuclei and heavy-particle-electron couplings [29,30] or by considering an alternative source related to unphysical meaning of the observed minima [23–26], no definitive explanation has been reached.

In the present work, we revisit the  $He^{2+}$ -He collisions in the framework of a nonperturbative semiclassical approach in combination with Eikonal approximation to calculate the SDCS taking into account the electron-electron correlations. Our main attention will be addressed to the issue surrounding the origin of such minima. This is achieved by evoking a detailed analysis based on Fraunhofer-type diffraction effects in connection with single capture (SC) and double capture

(DC) processes in the energy range 10–60 keV/u (0.63–1.55 a.u.). As we shall show later, our investigation can be viewed as an analogy to spatial Fraunhofer's diffraction patterns found in classical optics, and we believe that this picture makes evident the origin of the observed structures. We will extend our results and show that such structures are also present in asymmetry  $H^+$ -He collisions. Since we observe the scattering patterns in two different collision systems, the mechanism appears to be a general feature of ion-atom collisions.

This paper is organized as follows. In Sec. II we present a short description of the theoretical formalism adopted to study the collision processes under considerations. Section III is devoted to the detailed analysis of SDCSs and direct comparisons with experimental data. In the following, atomic units will be used except where otherwise stated.

## II. THEORY METHOD

We employ the semiclassical close-coupling approach of atomic collisions [32] to solve the time-dependent Schrödinger equation within double active electrons (see Ref. [33] and references therein, for detailed insight into the method). Briefly, the time-dependent wave function is expanded in terms of Gaussian-type orbitals (GTOs) on each center (projectile and atomic target at infinite separation), each with appropriate plane-wave translational factors to take into account the relative motion of the two collisions partners and ensure Galilean invariance of the results.

In the present close-coupling calculations, we have used the same sets of GTOs as in Refs. [33,34] to describe the species He,  $He^+$ , H, and  $H^-$ . In order to check the accuracy and convergence of this basis set, we have checked the state-selective capture probabilities by using a larger basis set, and it is found that both sets calculation are closed.

For the scattering calculations, we use an Eikonal approximation [35,36] to obtain the differential cross sections depending on scattering angle. For an inelastic transition the latter can be written in the center-of-mass frame, at a given angle  $\theta$ , as

$$\left. \frac{d\sigma}{d\Omega} \right|_{CM} = |A_{fi}|^2, \quad (1)$$

where the quantal scattering amplitudes  $A_{fi}$

$$A_{fi}(\Omega) = \beta \int_0^{+\infty} b db J_{|m_f - m_i|}(2\mu v \sin(\theta/2)) a_{fi}(b, +\infty) \quad (2)$$

are determined in turn from the impact-parameter-dependent transition amplitude  $a_{fi}$ . Here  $\beta = \mu v (-1)^{m_f - m_i + 1}$ ,  $\mu$  is the reduced mass,  $v$  is the relative collision velocity, and  $m_f$  ( $m_i$ ) is the magnetic quantum number of the final (initial) state. The function  $J$  denotes a Bessel function of the first kind. The semiclassical scattering amplitude  $a_{fi} = \tilde{a}_{fi} e^{2i(Z_T Z_P/v) \ln b}$  can be decomposed into an electronic part that is stemming from the coupled equation in the close-coupling approach for the transition amplitude  $\tilde{a}_{fi}$ . The second part corresponds to the nuclear contribution that is due to the Coulomb repulsion between the two nuclei. In the last expression,  $Z_T$  and  $Z_P$  are the core charges of the target and the projectile, respectively.

The SDCSs in the laboratory frame are related to those in the center-of-mass frame by

$$\left. \frac{d\sigma}{d\Omega} \right|_{CM} = \left[ \frac{(1 + 2\zeta \cos \theta + \zeta^2)^{3/2}}{1 + \zeta \cos \theta} \right] \left. \frac{d\sigma}{d\Omega} \right|_{CM}, \quad (3)$$

where  $\zeta = M_P/M_T$  is the ratio of the mass of the projectile  $M_P$  and target nuclei  $M_T$ . The scattering angles in the laboratory frame can be deduced from those in the center-of-mass frame

$$\tan \theta_{Lab} = \frac{\sin \theta}{\zeta + \cos \theta}. \quad (4)$$

In order to check the convergence of the SDCSs, we have evaluated the cross sections by integrating the SDCSs over scattering angles and compared with those obtained from integrating the electron capture probabilities over impact parameters. Within this procedure the results obtained are identical.

We note that expression (2) is reminiscent of the angular distribution of light of wave vector  $\vec{k}$ , when it is diffracted by a circular aperture in an infinite opaque screen. This phenomenon is well known in classical optics by the Fraunhofer-type diffraction of light, and its scattering amplitude is given by [37]

$$f(\theta) \propto \int_0^{+\infty} b db J_0[2k \sin(\theta/2)] g(b), \quad (5)$$

where  $g(b)$  is a pupil function reflecting the radial transmittance and phase shift of the aperture. This function is, for an ideal system (i.e., the light is merely transmitted), equal to one at every point within the pupil, and zero out within it. In these conditions, the latter expression takes the explicit form

$$f(\theta) \propto \frac{J_1(k\rho\theta)}{k\rho\theta}, \quad (6)$$

where  $\rho$  is the radius of the aperture.

The expression (2) provides the analogy between the collision of charged ions on atoms and Fraunhofer-type diffraction of light. This analogy was evoked in Ref. [38] (see also Ref. [34]). The similarity in both expressions (2) and (5) requires that  $m_f = m_i$  and demonstrates that the collision mechanisms can play a role analogous to that of an aperture in light diffraction. We will illustrate this analogy by evoking different state-selective capture SDCSs at different projectile energies.

## III. RESULTS AND DISCUSSION

In our scenario presented here, the de Broglie wavelength of the incoming projectile wave ( ${}^3He^{2+}$ ) is  $\lambda_{dB} = \frac{2\pi}{\mu v} \approx 0.0016$  a.u., and its value in the laboratory frame is  $9.01 \times 10^{-4}$  a.u. (corresponds to the projectile energy 40 keV/u). This wave propagates with the relative wave vector  $\vec{k}_i$  through the atomic target (He) and catches a two-electron into  $1s^2$ , then it scatters off with the final wave vector  $\vec{k}_f$  as sketched in Fig. 1.

Such scattering patterns are shown in Fig. 2(a) and exhibit ring structures in close analogy to spatial diffraction patterns found in classical optics. The observed structures become clear when the SDCSs are displayed in one-dimensional scattering [cf. Fig. 2(b)] and exhibit a minimum following by a maximum in scattering angles, in good agreement with the experimental

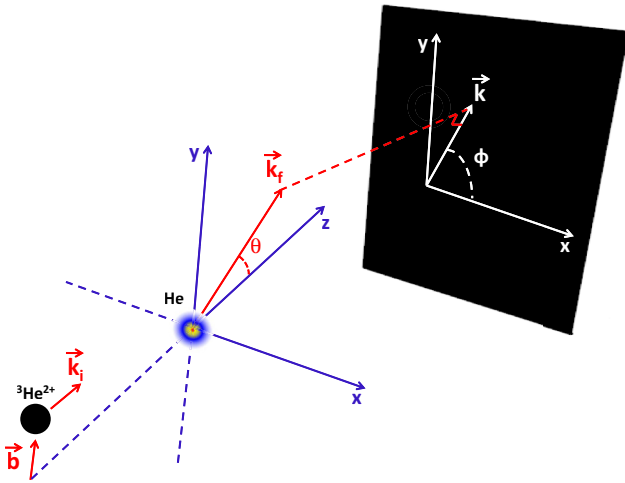


FIG. 1. (Color online) Scenario of the scattering of a moving  ${}^3\text{He}^{2+}$  and a helium atomic He, characterized by initial (final) wave vector and momentum transfer  $\vec{k}_i$  ( $\vec{k}_f$ ) and  $\vec{k}$ , respectively.  $\theta$  and  $\phi$  are the scattering polar and azimuthal angles, respectively.

data [39]. Such structures become more pronounced when the SDCSs are weighted by the  $\sin \theta_{\text{Lab}}$ , as illustrated in the inset of Fig. 2(b).

The validity of our interpretation of the features in the calculated results as being due to Fraunhofer diffraction is illustrated by comparing the theoretical distribution for such phenomena on the optical analogy with that obtained by SDCSs. The theoretical scattering angles of the first dark and first bright fringes are given by  $0.61\lambda_{dB}/\rho$  and  $0.819\lambda_{dB}/\rho$ , respectively [37], where  $\rho$  is the aperture radius. In the present analogy, the latter is closely related to the radius of the interaction region and can be deduced directly from the angular spacing between the first minima and maxima using Fraunhofer-type diffraction conditions (i.e.,  $\Delta\theta = 0.209\lambda_{dB}/\rho$ ). A similar procedure has been adopted in the work of Gudmundsson *et al.* [7], in which the radius of the aperture was chosen to reproduce position of the first minima in the measured SDCSs. In the present work, once the value  $\Delta\theta$  is deduced from our data presented in Fig. 2(b) (the first minima is located at  $\theta_{\text{Lab}} \approx 0.25$  mrad, and the first maxima at  $\theta_{\text{Lab}} \approx 0.34$  mrad), an effective radius is calculated and the obtained value is  $\rho \approx 2.1$  a.u.. It is found out that this value is quite close to a rough estimate of the value of the impact-parameter  $b$  beyond which the probability of electron capture  $P(b)$  is negligibly small, as indicated in Fig. 2(c) by red arrow.

Our demonstration of the origin of this phenomenon is supported by the picture of the DC-electron probabilities [cf. Fig. 2(c)]. The latter distribution is akin to a pupil function in optical analogy, and as expected no indication of an oscillatory structure is observed. This rules out such an interpretation related to the electronic behavior such as transient molecule formed by the passing  $\text{He}^{2+}$  ion and the He atom. Here we suggest an alternative explanation in terms of the scattered matter wave of the projectile on an atomic target. This is illustrated by considering the classical picture of the SDCSs as shown in Fig. 2(b) with dashed lines: the results stem from

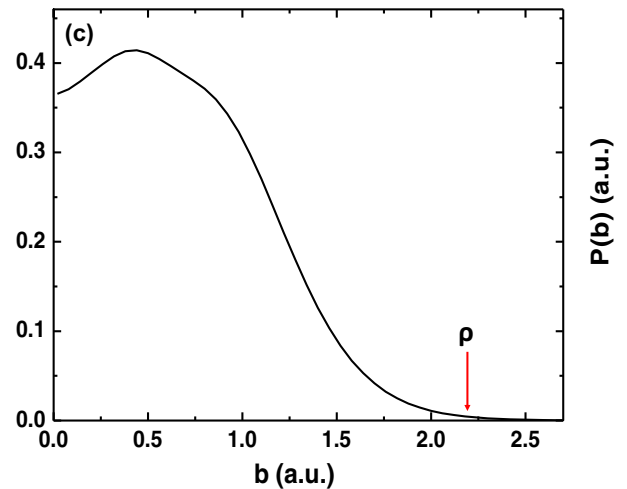
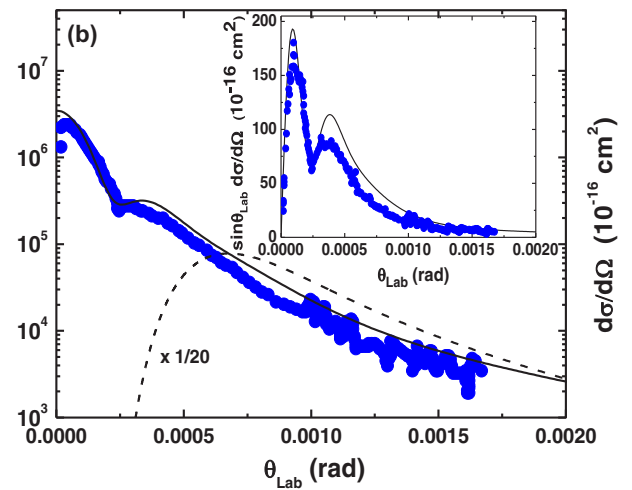
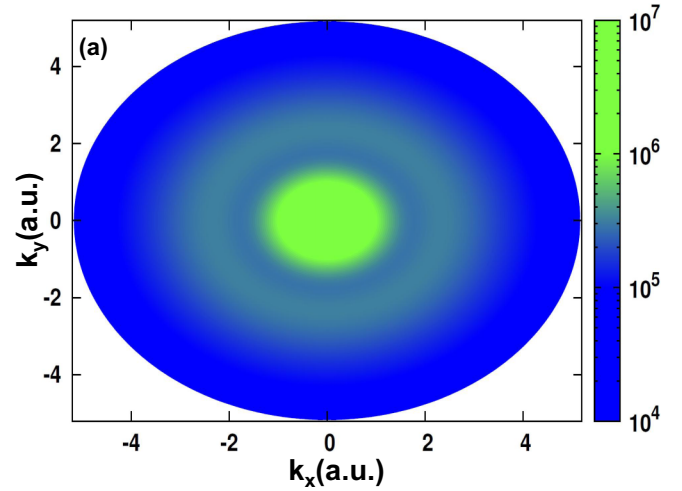


FIG. 2. (Color online) Calculations for DC into  $1s^2$  for 40 keV/u  ${}^3\text{He}^{2+}$ -He collisions. (a) Scattering pattern in momentum space in the plane perpendicular to the projectile direction (cf. Fig. 1) in the laboratory system. (b) SDCSs in one-dimensional scattering angles: (solid curve) our exact calculation is based on Eq. (2); (dashed curve) results stemming from the classical formula (7) and divided by 20; (full circle) experiment of Schöffler [39]. Inset: SDCS weighted by  $\sin \theta_{\text{Lab}}$ . (c) DC-electron capture probabilities. Red arrow indicates a rough estimate of the radius of the interaction region.

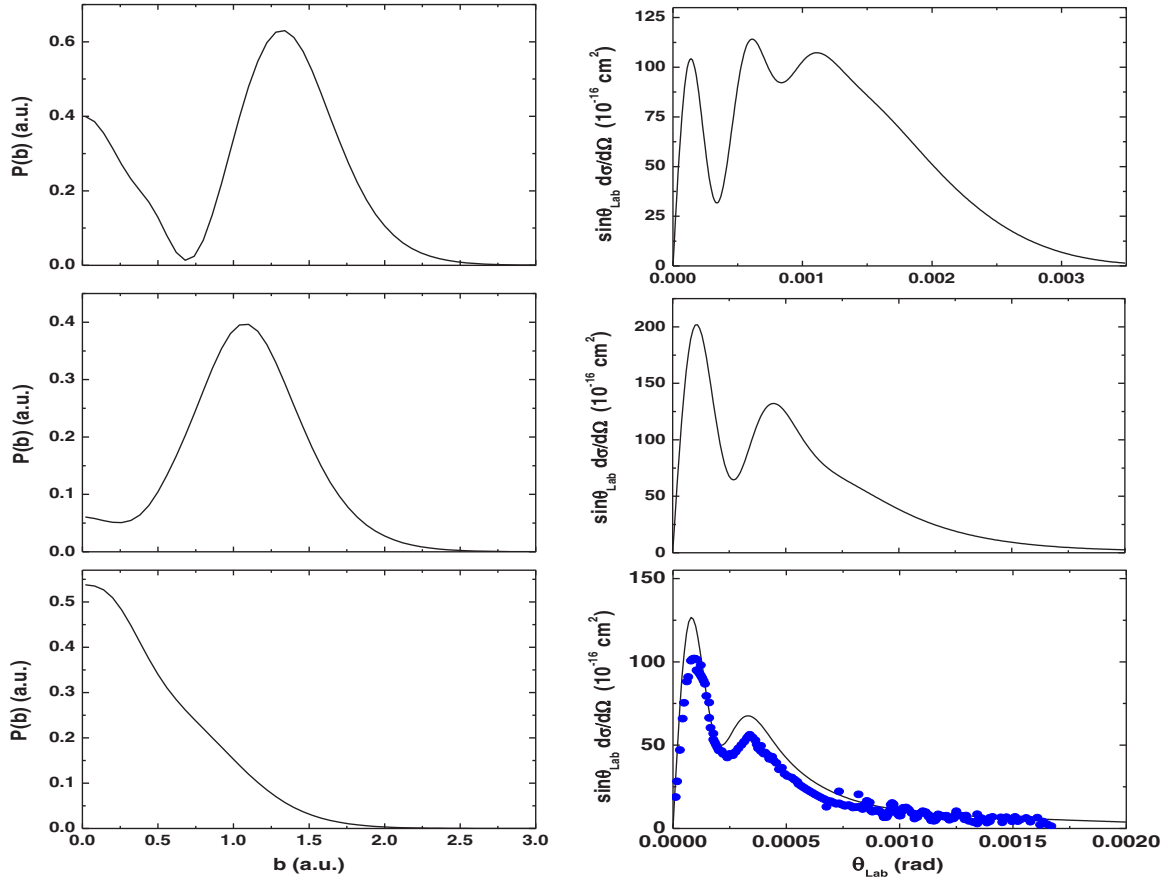


FIG. 3. (Color online) Calculations for DC into  $1s^2$  at three energies 10, 25, and 60 keV/u  ${}^3\text{He}^{2+}$ -He collisions from top to bottom panels, respectively. Left panel: DC-electron probabilities. Right panel: Corresponding SDCS weighted by  $\sin\theta_{\text{Lab}}$  in the laboratory frame. (full circle) experiment of Schöffler *et al.* [27].

the classical formula [40]

$$\frac{d\sigma}{d\Omega} = |\tilde{a}_{fi}(b)|^2 \left( \frac{d\sigma}{d\Omega} \right)_{\text{Ruth}}, \quad (7)$$

where  $\left( \frac{d\sigma}{d\Omega} \right)_{\text{Ruth}}$  is the Rutherford differential cross section for the classical elastic scattering of the nuclei, and  $b$  is given by the classical relation between scattering angle and impact parameter. It is obvious that the latter expression cannot lead to a complete information on the SDCS. This is owing to the classical description of the elastic scattering, which is not valid for small scattering angles [40]. Such lack of information is characterized by the nonreproduction of the expected effect by the classical calculation. We note that similar behavior has been observed in previous works [28,40,41].

At this point we conclude that our observations suggest that the observed structures result from the de Broglie matter-wave scattering of the projectile on the atomic target. This is consistent with our comprehensive picture resulting from our quantum SDCSs and supported by the shape of the probability distributions, which validates once again our interpretation in terms of diffraction phenomena, in analogy with Fraunhofer-type diffraction of light waves.

Let us now analyze the dependence of the observed minima and maxima with respect to the projectile energy. In Fig. 3 (on the right) our theoretical SDCSs weighted by  $\sin\theta_{\text{Lab}}$  are displayed together with some available experimental data [27]

for three projectile energies (from top to bottom) 10, 25, and 60 keV/u (the corresponding values of  $\lambda_{dB}$  in the laboratory frame are  $1.8 \times 10^{-3}$ ,  $1.14 \times 10^{-3}$ , and  $9.01 \times 10^{-4}$  a.u.) and the same electronic process as in Fig. 2. In the same figure (on the left) are plotted the corresponding probability distributions  $P(b)$ . As in Fig. 2, the latter distribution allows us to determine a rough estimate of the radius of the interaction region. It is found that the size of this narrow region decreases with increasing projectile energies. In parallel, the observed minima and maxima are shifted in scattering angles between the results. For the projectile energy 60 keV/u, the observed minima and maxima are well reproduced by the recent measurements of Schöffler *et al.* [27]. Their location for the three collision energies dealt with here are shown in Table I and are quite close to the values obtained in Fraunhofer diffraction theory (FDT) in classical optics.

These data demonstrate a connection between the radius and the projectile energy and illustrate how it affects the location of such minima and maxima. This behavior is closely analogous to that expected in classical optics, in which such location is proportional to the ratio of wavelength to radius of the aperture. Therefore, the projectile energy affects significantly the observed pattern and plays a crucial role in the formation of the predicted phenomenon.

In Fig. 4 we present results for the same system as in Fig. 3 and three different SC channels at the fixed collision energy

TABLE I. Position of fringes deduced from SDCS for DC into  $1s^2$  in the system  ${}^3\text{He}^{2+}\text{-He}$  and the corresponding values predicted by FDT at different projectile energies.

$E$ (keV/u)	Fringes	SDCS (mrad)	FDT (mrad)
10	1st dark	0.35	0.4
	1st bright	0.56	0.55
	2nd dark	0.8	0.74
	2nd bright	1.0	0.9
25	1st dark	0.28	0.28
	1st bright	0.4	0.37
60	1st dark	0.25	0.22
	1st bright	0.32	0.3

60 keV/u: SC to  $1s$  (top panels), SC to  $2s$  (middle panels), and SC to  $3s$  (bottom panels). Again similar diffraction profile is observed for the three SC channels, in excellent agreement with the measurements of Schöffler *et al.* [27]. Although the SDCSs exhibit similar behavior for such capture states, their amplitudes are much smaller for  $2s$  and  $3s$  states than those

TABLE II. Angular spacing deduced from SDCs for SC to  $1s$ ,  $2s$ , and  $3s$  in 60 keV/u  ${}^3\text{He}^{2+}\text{-He}$  collisions and the corresponding radius of the interaction region predicted by FDT.

State-selective SC	$1s$	$2s$	$3s$
Angular spacing (mrad) (SDCS)	0.04	0.05	0.04
Radius $\rho$ (a.u.) (FDT)	3.8	3.1	3.8

for  $1s$ . The observed difference is resulting from the smaller cross sections for  $2s$  and  $3s$  compared to those for  $1s$ , which can be seen clearly in the picture of SC-electron probabilities. Additionally, the observed diffraction signals show only slight variations in scattering angles depending upon the capture states. This is consistent with their dependence on the radius of the interaction region, which seems in turn to be varied slightly. This dependence is illustrated in the Table II in which the angular spacing for the three SC channels are listed together with the radius of the interaction region deduced from FDT to reproduce the first minima and maxima in the SDCSs.

These observations provide, therefore, an additional feature of atomic profile of diffraction of a projectile de Broglie matter wave related to the role of the radius of the narrow region, in analogy with Fraunhofer diffraction phenomena.

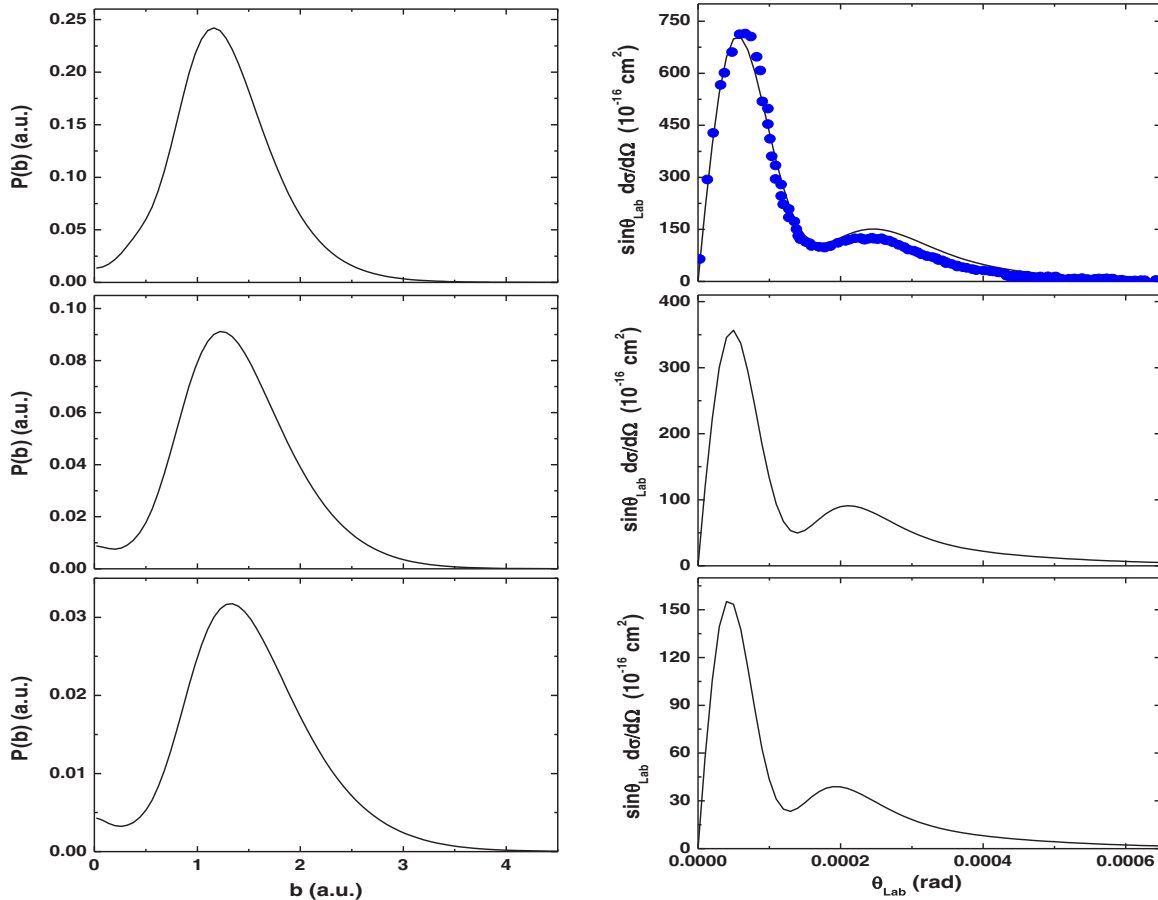


FIG. 4. (Color online) Calculations at energies 60 keV/u  ${}^3\text{He}^{2+}\text{-He}$  collisions for SC into  $1s$ ,  $2s$ , and  $3s$  from top to bottom panels, respectively. Left panel: SC-electron probabilities. Right panel: Corresponding SDCSs weighted by  $\sin\theta_{\text{Lab}}$  in the laboratory frame. Full circle: Experiment of Schöffler *et al.* [27].

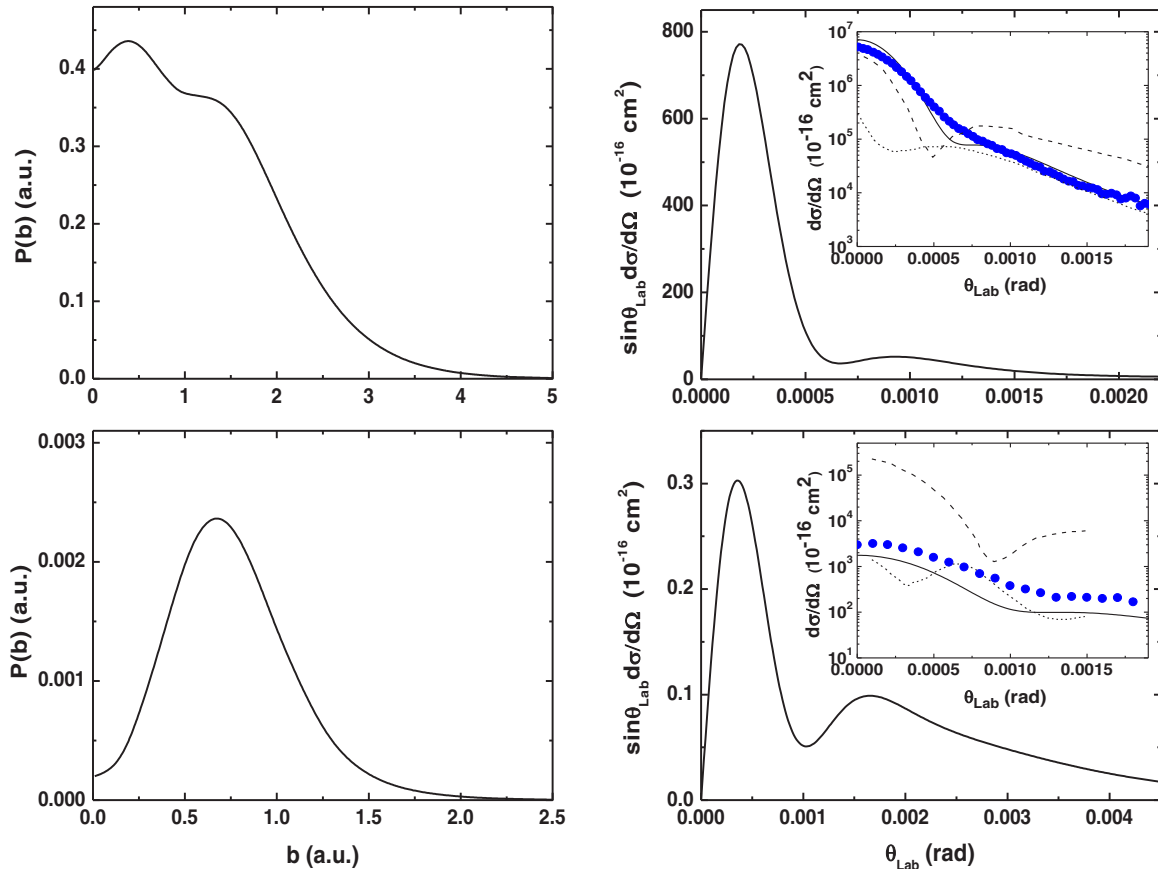


FIG. 5. (Color online) Calculations at energy 25 keV/u  $\text{H}^+$ -He collisions for SC to  $1s$  (top panels) and DC into  $1s^2$  (bottom panels). Left panel: Electron-capture probabilities. Right panel: Corresponding SDCS weighted by  $\sin\theta_{\text{Lab}}$  in the laboratory frame. Inset: Total SDCS vs scattering angles in laboratory frame. Dashed lines: Calculation of Harris *et al.* [24]. Short dashed lines: Calculation of Chowdhury *et al.* [26]. Full circle: Experimental data of Schulz *et al.* [29].

In order to make conclusions about the general features of the observed phenomenon in energetic ion-atom collisions, we extend our study to an asymmetric system. Interestingly, similar structure prevails also in a 25 keV  $\text{H}^+$ -He collision system and for the two evoked capture channels (cf. Fig. 5): SC to  $1s$  and DC into  $1s^2$ . However, it is found out that summation of the SDCS over the bound states of the projectile can wash out the observed structure. Similar observations were reported experimentally by Mergel *et al.* [42] for swift ion-atom collisions. Indeed, the observed structure in DC into  $1s^2$  disappears in the total DC process [cf. inset of Fig. 5 (bottom panel)], which is due to the destructive interferences between the bound states involving  $\text{H}^-$  in SDCSs. In contrast, such structures remain clear in the total SC [cf. inset of Fig. 5 (top panel)]. This is because the  $1s$  state capture is the dominant channel in the system considered here. Our results compare well with the measurements of Schulz *et al.* [29], except for DC where they are small in the magnitude by a factor of 2. However, their shape is reproduced almost perfectly. In contrast, the recent calculations based on perturbative approach [24,26] show a serious disagreement in both magnitude and shape of the SDCS (cf. insets of Fig. 5).

The close agreement between our nonperturbative calculations and the experimental data, on the one hand, and those based on Fraunhofer-type diffraction theory, on the

other, supports our interpretation of the origin of the observed structure.

Although diffraction-like oscillations are well known as a general feature of charge exchange in scattering theory of ion-atom collisions [35], most of them were observed at slow collision energies and often termed either “Stueckelberg oscillations” [43,44] or resulting from the number of times that the active electron moves between nuclear centers [45,46]. At the energy range considered here both explanations are unlikely and an alternative source is required. This is reached in the present work by evoking an asymmetric and symmetric ion-atom system, in which Fraunhofer-type diffraction effects are observed clearly and interpreted in terms of the de Broglie matter wave of the scattering projectile on the atomic target.

#### IV. CONCLUSIONS

In conclusion we have presented a semiclassical close-coupling approach in combination with an Eikonal approximation to calculate the SDCS. We have found excellent agreement with available experimental data over a broad range of impact energies considered here. Our study provides a complete theoretical demonstration of Fraunhofer-type diffraction in connection with DC and SC in intermediate  ${}^3\text{He}^{2+}$ -He and  $\text{H}^+$ -He collisions involving correlated two active electrons. It

was found that the SDCSs exhibit a behavior closely analogous to the intensity distribution obtained in Fraunhofer diffraction theory in classical optics. Such an analogy was supported by further analysis of the SDCSs, which gave evidence for coherent matter-wave scattering of the projectile from atoms via electron transfer processes.

A demonstration of the origin of the observed phenomenon was provided by an additional calculation based on classical elastic scattering, and supported by the shape of the probability distribution. The latter enables us to determine the radius of the interaction region, which plays a crucial role in the predicted phenomena. We have emphasized this role by evoking different capture channels in which the narrow regions of the probability distributions can be affected. It was found that such study shows only slight variations of the observed fringes, which is

consistent with the observed modifications of the radius. In addition, we have analyzed the dependence of the predicted phenomena with respect to the projectile energy: since as the projectile velocity increases the de Broglie wavelength decreases, hence the density of oscillation patterns gets higher. Extending this to an asymmetric system reveals a similar effect and demonstrates a general feature of the de Broglie matter wave of the scattering projectile on the atomic target, in analogy with Fraunhofer-type diffraction of light.

#### ACKNOWLEDGMENTS

The author thanks Prof. Jan Petter Hansen for comments that greatly improved the paper. This work was supported by the FP7-PEOPLE-2010-IRSES program 269243 DWBQS.

- 
- [1] N. Stolterfoht, B. Sulik, V. Hoffmann, B. Skogvall, J. Y. Chesnel, J. Rangama, F. Frémont, D. Hennecart, A. Cassimi, X. Husson, A. L. Landers, J. A. Tanis, M. E. Galassi, and R. D. Rivarola, *Phys. Rev. Lett.* **87**, 023201 (2001).
- [2] L. Ph. H. Schmidt, S. Schössler, F. Afaneh, M. Schöffler, K. E. Stiebing, H. Schmidt-Böcking, and R. Dörner, *Phys. Rev. Lett.* **101**, 173202 (2008).
- [3] D. Misra, H. T. Schmidt, M. Gudmundsson, D. Fischer, N. Haag, H. A. B. Johansson, A. Källberg, B. Najjari, P. Reinhed, R. Schuch, M. Schöffler, A. Simonsson, A. B. Voitkiv, and H. Cederquist, *Phys. Rev. Lett.* **102**, 153201 (2009).
- [4] M. van der Poel, C. V. Nielsen, M.-A. Gearba, and N. Andersen, *Phys. Rev. Lett.* **87**, 123201 (2001).
- [5] M. van der Poel, C. V. Nielsen, M. Rybaltov, S. E. Nielsen, M. Machholm, and N. Andersen, *J. Phys. B: At. Mol. Opt. Phys.* **35**, 4491 (2002).
- [6] Q. Wang, X. Ma, X. L. Zhu, and S. F. Zhang, *J. Phys. B: At. Mol. Opt. Phys.* **45**, 025202 (2012).
- [7] M. Gudmundsson, D. Fischer, N. Haag, H. A. B. Johansson, D. Misra, P. Reinhed, H. Schmidt-Böcking, R. Schuch, M. Schöffler, K. Stöckel, H. T. Schmidt, and H. Cederquist, *J. Phys. B: At. Mol. Opt. Phys.* **43**, 185209 (2010).
- [8] S. Sharma, A. Hasan, K. N. Egodapitiya, T. P. Arthanayaka, G. Sakhelashvili, and M. Schulz, *Phys. Rev. A* **86**, 022706 (2012).
- [9] W. Fritsch and C. D. Lin, *Phys. Rev. A* **54**, 4931 (1996).
- [10] C. H. Liu, J. G. Wang, and R. K. Janev, *J. Phys. B: At. Mol. Opt. Phys.* **45**, 235203 (2012).
- [11] I. Mančev, *J. Phys. B: At. Mol. Opt. Phys.* **36**, 93 (2003).
- [12] I. Mančev, V. Mergel, and L. Schmidt, *J. Phys. B: At. Mol. Opt. Phys.* **36**, 2733 (2003).
- [13] D. Belkić, *Quantum Theory of High-Energy Ion-Atom Collisions* (Taylor and Francis, London, 2008).
- [14] E. Ghanbari-Adivi, *J. Phys. B: At. Mol. Opt. Phys.* **44**, 165204 (2011).
- [15] M. S. Schöffler, H.-K. Kim, O. Chuluunbaatar, S. Houamer, A. G. Galstyan, J. N. Titze, T. Jahnke, L. Ph. H. Schmidt, H. Schmidt-Böcking, R. Dörner, Yu. V. Popov, and A. A. Bulychev, *Phys. Rev. A* **89**, 032707 (2014).
- [16] J. G. Lockwood, H. F. Helbig, and E. Everhart, *Phys. Rev.* **132**, 2078 (1963).
- [17] D. Bordenave-Montesquieu and R. Dagnac, *J. Phys. B: At. Mol. Opt. Phys.* **25**, 2573 (1992).
- [18] L. H. Thomas, *Proc. R. Soc. Lond.* **114**, 561 (1927).
- [19] E. Horsdal-Pedersen, C. L. Cocke, and M. Stockli, *Phys. Rev. Lett.* **50**, 1910 (1983).
- [20] H. Vogt, R. Schuch, E. Justiniano, M. Schulz, and W. Schwab, *Phys. Rev. Lett.* **57**, 2256 (1986).
- [21] D. Fischer, M. Gudmundsson, Z. Berényi, N. Haag, H. A. B. Johansson, D. Misra, P. Reinhed, A. Källberg, A. Simonsson, K. Stöckel, H. Cederquist, and H. T. Schmidt, *Phys. Rev. A* **81**, 012714 (2010).
- [22] M. Zapukhlyak and T. Kirchner, *Phys. Rev. A* **80**, 062705 (2009).
- [23] A. L. Harris, J. L. Peacher, D. H. Madison, and J. Colgan, *Phys. Rev. A* **80**, 062707 (2009).
- [24] A. L. Harris, J. L. Peacher, and D. H. Madison, *Phys. Rev. A* **82**, 022714 (2010).
- [25] U. Chowdhury, A. L. Harris, J. L. Peacher, and D. H. Madison, *J. Phys. B: At. Mol. Opt. Phys.* **45**, 035203 (2012).
- [26] U. Chowdhury, A. L. Harris, J. L. Peacher, and D. H. Madison, *J. Phys. B: At. Mol. Opt. Phys.* **45**, 175204 (2012).
- [27] M. S. Schöffler, J. Titze, L. Ph. H. Schmidt, T. Jahnke, N. Neumann, O. Jagutzki, H. Schmidt-Böcking, R. Dörner, and I. Mančev, *Phys. Rev. A* **79**, 064701 (2009).
- [28] A. Hasan, B. Tooke, M. Zapukhlyak, T. Kirchner, and M. Schulz, *Phys. Rev. A* **74**, 032703 (2006).
- [29] M. Schulz, T. Vajnai, and J. A. Brand, *Phys. Rev. A* **75**, 022717 (2007).
- [30] M. Zapukhlyak, T. Kirchner, A. Hasan, B. Tooke, and M. Schulz, *Phys. Rev. A* **77**, 012720 (2008).
- [31] M. S. Schöffler, J. N. Titze, L. Ph. H. Schmidt, T. Jahnke, O. Jagutzki, H. Schmidt-Böcking, and R. Dörner, *Phys. Rev. A* **80**, 042702 (2009).
- [32] W. Fritsch and C. D. Lin, *Phys. Rep.* **202**, 1 (1991).
- [33] N. Sisourat, I. Piskog, and A. Dubois, *Phys. Rev. A* **84**, 052722 (2011).
- [34] H. Agueny, Ph.D. thesis, Université Paris-Sorbonne, Paris IV, 2014; <https://hal.inria.fr/LCPMR/tel-01052860v1>.
- [35] B. H. Bransden and M. R. C. McDowell, *Charge Exchange and the Theory of Ion-Atom Collisions* (Clarendon Press, Oxford, 1992).

- [36] A. Dubois, S. E. Nielsen, and J. P. Hansen, *J. Phys. B: At. Mol. Opt. Phys.* **26**, 705 (1993).
- [37] M. Born and E. Wolf, *Principles of Optics: Electromagnetic Theory of Propagation, Interference and Diffraction of Light*, 7th ed. (Cambridge University Press, Cambridge, 2003), pp. 421–429.
- [38] L. Wilets and S. J. Wallace, *Phys. Rev.* **169**, 84 (1968).
- [39] M. Schöffler, Ph.D. thesis, Johann Wolfgang Goethe Universität, Frankfurt am Main, 2006; <http://publikationen.ub.uni-frankfurt.de/volltexte/2006/3536/>.
- [40] P. T. Greenland, *J. Phys. B: At. Mol. Phys.* **14**, 3707 (1981).
- [41] J. E. Miraglia, R. D. Piacentini, R. D. Rivarola, and A. Salin, *J. Phys. B: At. Mol. Phys.* **14**, L197 (1981).
- [42] V. Mergel, R. Dörner, J. Ullrich, O. Jagutzki, S. Lencinas, S. Nüttgens, L. Spielberger, M. Unverzagt, C. L. Cocke, R. E. Olson, M. Schulz, U. Buck, E. Zanger, W. Theisinger, M. Isser, S. Geis, and H. Schmidt-Böcking, *Phys. Rev. Lett.* **74**, 2200 (1995).
- [43] R. E. Olson and F. T. Smith, *Phys. Rev. A* **3**, 1607 (1971).
- [44] A. Barany, H. Danared, H. Cederquist, P. Hvelplund, H. Knudsen, J. O. K. Pedersen, C. L. Cocke, L. N. Tunnell, W. Waggoner, and J. P. Giese, *J. Phys. B* **19**, L427 (1986).
- [45] S. Otranto, I. Blank, R. E. Olson, and R. Hoekstra, *J. Phys. B* **45**, 175201 (2012).
- [46] I. Blank, S. Otranto, C. Meinema, R. E. Olson, and R. Hoekstra, *Phys. Rev. A* **87**, 032712 (2013).